of spikes fired by a neuron in each spatio-temporal bin (spatial width 1 pixel = 0.66 cm, temporal width 1° ≈ 0.35 ms) by the total time spent by the rat in that bin. The result was smoothed by convolution with a two-dimensional gaussian (spatial width 2.4 cm, temporal width 12° ≈ 4.2 ms).

Received 24 October 2001; accepted 22 April 2002; doi:10.1038/nature00807.

1. Markram, H., Lubke, J., Frotscher, M. & Sakmann, B. Regulation of synaptic efficacy by coincidence of postsynaptic APs and EPSPs. *Science* **275,** 213–215 (1997).
2. Bi, G. Q. & Poo, M. M. Synaptic modifications in cultured hippocampal neurons: dependence on spike timing, synaptic strength, and postsynaptic cell type. *J. Neurosci.* **18,** 10464–10472 (1998).
3. O'Keefe, J. & Dostrovsky, J. The hippocampus as a spatial map. Preliminary evidence from unit activity in the freely-moving rat. *Brain Res.* **34,** 171–175 (1971).
4. Wilson, M. A. & McNaughton, B. L. Dynamics of the hippocampal ensemble code for space. *Science* **261,** 1055–1058 (1993).
5. O'Keefe, J. & Recce, M. L. Phase relationship between hippocampal place units and the EEG theta rhythm. *Hippocampus* **3,** 317–330 (1993).
6. Skaggs, W. E., McNaughton, B. L., Wilson, M. A. & Barnes, C. A. Theta phase precession in hippocampal neuronal populations and the compression of temporal sequences. *Hippocampus* **6,** 149–172 (1996).
7. Hopfield, J. J. Pattern recognition computation using action potential timing for stimulus representation. *Nature* **376,** 33–36 (1995).
8. Tsodyks, M. V., Skaggs, W. E., Sejnowski, T. J. & McNaughton, B. L. Population dynamics and theta rhythm phase precession of hippocampal place cell firing: a spiking neuron model. *Hippocampus* **6,** 271–280 (1996).
9. Wallenstein, G. V. & Hasselmo, M. E. GABAergic modulation of hippocampal population activity: sequence learning, place field development, and the phase precession effect. *J. Neurophysiol.* **78,** 393–408 (1997).
10. Kamondi, A., Acsady, L., Wang, X. J. & Buzsaki, G. Theta oscillations in somata and dendrites of hippocampal pyramidal cells in vivo: activity-dependent phase-precession of action potentials. *Hippocampus* **8,** 244–261 (1998).
11. Bose, A., Booth, V. & Recce, M. A temporal mechanism for generating the phase precession of hippocampal place cells. *J. Comput. Neurosci.* **9,** 5–30 (2000).
12. Mehta, M. R., Quirk, M. C. & Wilson, M. A. Experience-dependent asymmetric shape of hippocampal receptive fields. *Neuron* **25,** 707–715 (2000).
13. Toth, K., Freund, T. F. & Miles, R. Disinhibition of rat hippocampal pyramidal cells by GABAergic afferents from the septum. *J. Physiol.* **500,** 463–474 (1997).
14. Mehta, M. R. & Wilson, M. A. From hippocampus to V1: Effect of LTP on spatio-temporal dynamics of receptive fields. *Neurocomputing* **32,** 905–911 (2000).
15. Mehta, M. R. Neuronal dynamics of predictive coding. *Neuroscientist* **7,** 490–495 (2001).
16. Buzsaki, G., Rappelsberger, P. & Kellenyi, L. Depth profiles of hippocampal rhythmic slow activity ('theta rhythm') depend on behaviour. *Electroencephalogr. Clin. Neurophysiol.* **61,** 77–88 (1985).
17. Jensen, O. & Lisman, J. E. Hippocampal CA3 region predicts memory sequences: accounting for the phase precession of place cells. *Learn. Mem.* **3,** 279–287 (1996).
18. Hasselmo, M. E., Fransen, E., Dickson, C. & Alonso, A. A. Computational modeling of entorhinal cortex. *Ann. NY Acad. Sci.* **911,** 418–446 (2000).
19. Hirase, H., Czurko, H. H., Csicsvari, J. & Buzsaki, G. Firing rate and theta-phase coding by hippocampal pyramidal neurons during 'space clamping'. *Eur. J. Neurosci.* **11,** 4373–4380 (1999).
20. Ekstrom, A. D., Meltzer, J., McNaughton, B. L. & Barnes, C. A. NMDA receptor antagonism blocks experience-dependent expansion of hippocampal "place fields". *Neuron* **31,** 631–638 (2001).
21. Magee, J. C. Dendritic mechanisms of phase precession in hippocampal ca1 pyramidal neurons. *J. Neurophysiol.* **86,** 528–532 (2001).
22. Livingstone, M. S. Mechanisms of direction selectivity in macaque V1. *Neuron* **20,** 509–526 (1998).
23. Chance, F. S., Nelson, S. B. & Abbott, L. F. Synaptic depression and the temporal response characteristics of V1 cells. *J. Neurosci.* **18,** 4785–4799 (1998).
24. Rao, R. P. & Sejnowski, T. J. Predictive learning of temporal sequences in recurrent neocortical circuits. *Novartis Found. Symp.* **239,** 208–229 (2001).
25. Konig, P., Engel, A. K., Roelfsema, P. R. & Singer, W. How precise is neuronal synchronization? *Neural Comput.* **7,** 469–485 (1995).
26. Levy, W. B., in *Computational Models of Learning in Simple Neural Systems* (eds Hawkins, R. D. & Bower, J. H.) 243–305 (Academic, New York, 1989).
27. Blum, K. I. & Abbott, L. F. A model of spatial map formation in the hippocampus of the rat. *Neural Comput.* **8,** 85–93 (1996).
28. Mehta, M. R. & McNaughton, B. L. in *Computational Neuroscience: Trends in Research* (ed. Bower, J.) 741–745 (Plenum, New York, 1996).
29. Mehta, M. R., Barnes, C. A. & McNaughton, B. L. Experience-dependent, asymmetric expansion of hippocampal place fields. *Proc. Natl Acad. Sci. USA* **94,** 8918–8921 (1997).
30. Zar, J. H. *Biostatistical Analysis* (Prentice Hall, New Jersey, 1999).

Supplementary Information accompanies the paper on *Nature*'s website (http://www.nature.com/nature).

Acknowledgements

We thank W.F. Asaad, G. Liu, K. Louie, J. Raymond and S. Schnall for comments on the manuscript. This work was supported by the NIH (M.A.W.) and an HHMI pre-doctoral fellowship (A.K.L.). Parts of this work were presented at the Computational Neuroscience Meeting 2000 and at the Society for Neuroscience meeting 2001.

Competing interests statement

The authors declare that they have no competing financial interests.

Correspondence and requests for materials should be addressed to M.R.M. (e-mail: mayank@mit.edu) or M.A.W. (e-mail: wilson@cortical.mit.edu).

Modulation of virulence within a pathogenicity island in vancomycin-resistant *Enterococcus faecalis*

Nathan Shankar*, Arto S. Baghdayan* & Michael S. Gilmore†

** Department of Pharmaceutical Sciences and † Departments of Ophthalmology and Microbiology & Immunology, University of Oklahoma Health Sciences Center, PO Box 26901, Oklahoma City, Oklahoma 73190, USA*

Enterococci are members of the healthy human intestinal flora, but are also leading causes of highly antibiotic-resistant, hospital-acquired infection[1]. We examined the genomes of a strain of *Enterococcus faecalis* that caused an infectious outbreak in a hospital ward in the mid-1980s (ref. 2), and a strain that was identified as the first vancomycin-resistant isolate in the United States[3], and found that virulence determinants were clustered on a large pathogenicity island, a genetic element previously unknown in this genus. The pathogenicity island, which varies only subtly between strains, is approximately 150 kilobases in size, has a lower G + C content than the rest of the genome, and is flanked by terminal repeats. Here we show that subtle variations within the structure of the pathogenicity island enable strains harbouring the element to modulate virulence, and that these variations occur at high frequency. Moreover, the enterococcal pathogenicity island, in addition to coding for most known auxiliary traits that enhance virulence of the organism, includes a number of additional, previously unstudied genes that are rare in non-infection-derived isolates, identifying a class of new targets associated with disease which are not essential for the commensal behaviour of the organism.

In a study of a hospital ward epidemic in the mid-1980s, one *E. faecalis* strain resistant to many different antibiotics was identified as having caused over 30 infections (typified by isolate MMH594) and carried a fivefold increased risk of death within 3 weeks of isolation[2]. Several years later, the first vancomycin-resistant enterococcal isolate in the United States was identified approximately 400 miles away, and serial isolates (V583 and V586) were obtained from a chronically infected patient[3]. The vancomycin-resistance determinant has been characterized in molecular detail[4], and strain V583 was provided for genome analysis (for strain V583 genome data see http://www.tigr.org/tigr-scripts/CMR2/GenomePage3.spl?database = gef).

We and others have analysed a number of virulence factors in *E. faecalis*, including a structurally novel toxin, the cytolysin[5–7], and a surface protein, Esp[8], which contributes to colonization of the bladder in a model of urinary tract infection[9]. Esp confers biofilm production capability to enterococci[10], and a highly conserved Esp variant is common among clinical vancomycin-resistant and vancomycin-sensitive *E. faecium* strains[11–13]. *Enterococcus faecalis* strains V583 and V586 were isolated from a patient 11 days apart[3], and initial studies failed to identify differences between these isolates as they exhibited what appeared to be identical DNA fingerprint patterns. However, subsequent experiments designed to localize genes coding for both Esp and cytolysin found them on the chromosome of V586, but not V583. The difference was localized to a relatively small deletion within a roughly 315 kilobase (kb) *Sfi*I fragment in V583 (Fig. 1), which suggested that *cyl* and *esp* are closely linked.

Alignment and comparison of nucleotide sequences coding for the cytolysin operon, *esp* and surrounding regions of the V586 genome (Esp^+, Cyl^-), and the point of deletion of these functions in the genome of V583 (Esp^-, Cyl^-), (see http://www.tigr.org/tigr-scripts/CMR2/GenomePage3.spl?database = gef), revealed a

17,036-bp deletion in V583 (Fig. 2a), extending from within EF0047–EF0057 (see Supplementary Information Table 1). In the genome of V586, IS*256*- and IS*905*-like insertion elements (refs 14 and 15, respectively) occur within the cytolysin operon[6] in *cylB*, resulting in strain V586 being phenotypically non-cytolytic, although it harbours the entire cytolysin operon. An additional IS*905*-like element occurs in strain V586 at the distal end of the 17,036 bp segment, bracketing the *esp* gene and several other functions of unknown relevance to disease (Fig. 2a). Strain V583 (Esp^-, Cyl^-) was generated by spontaneous deletion of DNA from the V586 genome, beginning at the point of fusion between the IS*256*-like element and *cylB*, and ending at a point 17,036-bp downstream that occurs 276 bp in the 3′ direction to the distal IS*905*-like element, between direct repeats of a 5-bp sequence (Fig. 2b). The deletion resulting in strain V583 removed the 3′ half of the cytolysin operon and regions downstream, including the entire *esp* gene, rendering this strain deficient in expression of either of these virulence traits.

Quantitative polymerase chain reaction (PCR) revealed that precise excision of the 17,036-bp DNA segment from strain V586 (Esp^+, Cyl^-) occurs at a frequency of approximately 1 in 10^3 cells during overnight cultivation *in vitro*, a rate similar to that observed in modulation of virulence in other bacterial species by phase variation[16]. The mechanism for this specific, high frequency recombination is presently unknown, but it is suggestive of a highly evolved switch for modulating bacterial virulence. Strain V583 (Esp^-, Cyl^-) was the first of serial isolates, and is the strain that has undergone deletion. This suggests that either the patient was infected with a population of *E. faecalis* that was heterogeneous with respect to this deletion, or that deletion occurred on subsequent laboratory passage.

As *esp* and the cytolysin operon were co-localized on the chromosome of the isolate that had not undergone this spontaneous deletion, strain V586, it was of interest to determine whether they were also linked on the genome of strain MMH594 (Esp^+, Cyl^+), which caused multiple life-threatening infections at another healthcare centre several years earlier[2]. Hybridization and single-pass sequencing revealed that the region spanning cytolysin and *esp* genes on strain V586 (Fig. 2a) was nearly identical on the genome of MMH594, except for the absence of the IS*256*- and IS*905*- like elements that interrupt *cylB* in strain V586. MMH594 is therefore phenotypically Esp-positive and cytolytic, and seems to represent the prototype from which strains V586 and V583 evolved.

Nucleotide sequence similarities between the genomes of strain V586 and MMH594 did not end in the immediate vicinity of the cytolysin and *esp* genes, however, suggesting the presence of a larger common element on which these virulence traits reside. Primer walking was used to extend MMH594 and V586 sequence analysis in both directions outward from the point where Esp and cytolysin determinants were deleted in V583, until sequences that were shared by a non-infection-derived oral isolate of *E. faecalis*, strain OG1 (ref. 17), were encountered. These experiments identified an insertion of 153,571 bp of DNA in the genome of the clinical isolate MMH594 (GenBank accession number AF454824) with highly conserved variations in V586 and V583, which was absent from strain OG1. The point at which this large genetic element had inserted into the chromosomes of the clinical isolates occurred 3′ to a 10-bp sequence on the genome that was reiterated at the distal end of the element (Fig. 3a). Comparison of the element in MMH594 with those of V586 and V583 (Fig. 3b) revealed the accretion of additional IS elements in the latter isolates, and a 2.8-kb region

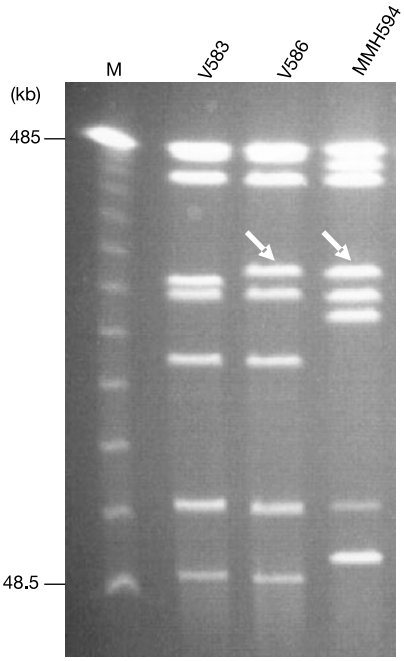

Figure 1 Pulsed-field gel electrophoretic (PFGE) banding patterns of S*fi*I-restricted genomic DNA[8]. Arrows point to the approximately 315-kb restriction fragment from V586 and MMH594 DNA to which probes for *esp* and *cylA* hybridize. Lane M is Lambda Ladder PFG marker from New England Biolabs.

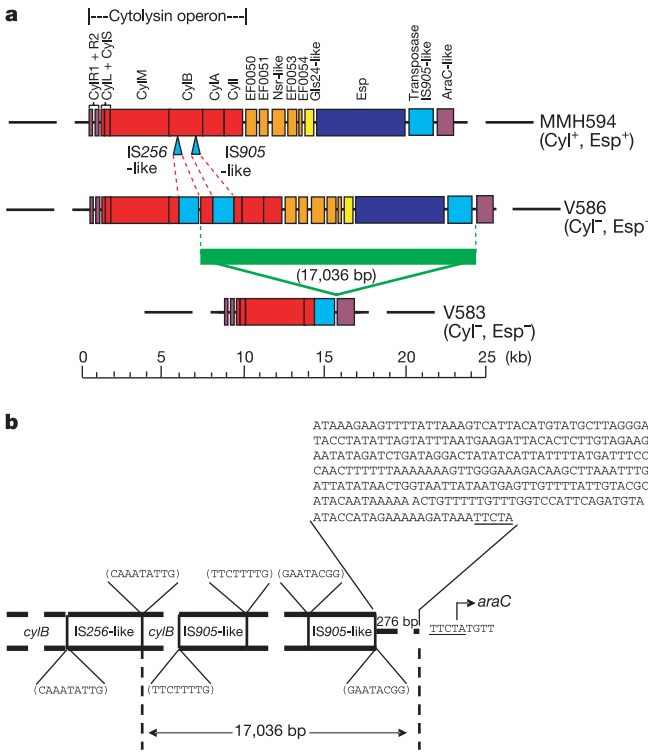

Figure 2 Schematic alignment and comparison of the genomic regions harbouring Esp, cytolysin and flanking functions within the PAI in MMH594, to similar regions in strains V586 and V583. **a**, The insertion sites for IS*256*- and IS*905*-like elements on the MMH594 chromosome, (insertions which result in the V586 phenotype) are shown by solid triangles. The region bounded by the dotted vertical lines denotes the 17,036-bp DNA segment that spontaneously excises out of the V586 chromosome resulting in V583. **b**, Junction sequences on the chromosome of V586 at the site of deletion of the 17,036-bp DNA segment. The 9- and 8-bp target sites duplicated after the insertion of the IS*256*- and IS*905*-like sequences are shown in parentheses. The 5-bp direct repeat at the right junction is underlined.

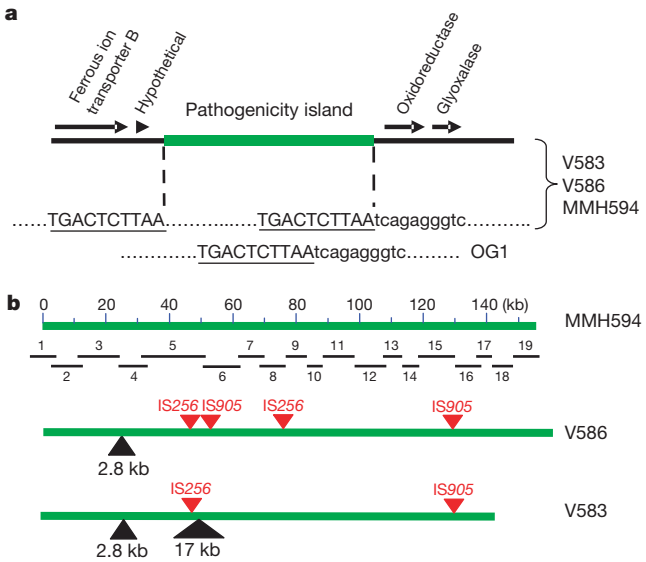

Figure 3 Junction sequences flanking the PAI in infection-derived isolates V583 (Esp^-, Cyl^-), V586 (Esp^+, Cyl^-) and MMH594 (Esp^+, Cyl^+). **a**, Primer pair PAI164 and PAI167 (see Methods) was used to PCR amplify a 2,121-bp segment of OG1 DNA spanning the predicted PAI insertion site and the product sequenced to confirm the point of insertion. The 10-bp duplicated sequence is underlined. **b**, Schematic alignment and comparison of the PAI in the three clinical isolates. The red triangles denote the locations of IS elements in strains V583 and V586, which are absent in MMH594. The black triangles represent regions present in MMH594 but missing from the V583 and V586 genomes. The 2.8-kb region specifies the location of a group II intron-like sequence. Numbered horizontal bars indicate overlapping regions of the PAI amplified from genomic DNA.

unique to MMH594. Notably, the 2.8-kb region in MMH594 possesses the features of a group II intron including consensus 5′ (GTGCG) and 3′(AT) splice sites[18], and a single reading frame coding for a homologue of the intron-coded protein IepA[19]. Excision of this intron would be predicted to generate an in-frame fusion of the 5′ and 3′ exons of *traG*[20] in strains V583 and V586. In contrast to the high-frequency deletion of the Esp and cytolysin-coding region from within the pathogenicity island (PAI) of V586, we determined by quantitative PCR that the PAI itself is integrated in a stable manner in the chromosomes of V583, V586 and MMH594, and does not undergo spontaneous deletion within the limits of detection.

The genetic element in MMH594 codes for 129 open reading frames (ORFs) (Fig. 4) and possesses the hallmarks of a PAI[21] including large size, terminal duplication at the target site, significantly variant G + C content of 32.2%, and the presence of genes that code for transposases, transcriptional regulators and proteins with known or potential roles in virulence or adaptation and survival in different environments. Virulence traits coded for within the *E. faecalis* PAI (Fig. 4 and Supplementary Information Table 1) include the aforementioned Esp and cytolysin, and also aggregation substance[22], which contributes to bacterial clumping, survival in neutrophils[23] and adherence to host tissues[24]. Additionally, within the element are genes that seem to code for a DNA-damage-inducible protein, an AraC-like transcriptional regulator, a conjugated bile acid hydrolase, components of the phosphotransferase system, and a Gls24-like starvation-inducible protein[25]; however, there are none that are known to code for antibiotic resistance. The PAI also codes for 18 ORFs for which no function could be predicted. The role of these genes and bacterial survival or proliferation in the unique environment encountered in a hospital, or at sites of infection, remains to be explored.

To test independently whether new traits not previously associated with known roles in enterococcal disease pathogenesis were truly elements of a pathogenicity island, or were randomly interspersed chromosomal genes of *E. faecalis*, we performed the following experiment. A panel of 40 clinical isolates from widely dispersed geographical sites, and 40 fecal isolates from healthy volunteers, were examined by hybridization for the presence of the detected *araC*-like regulator, the stress-inducible *gls24* homologue, and the inferred conjugated bile acid hydrolase (*cbh*). Clinical isolates were observed to be significantly enriched for all three genes: *araC*-like ($P < 0.001$), *cbh* ($P < 0.01$) and *gls24*-like ($P < 0.001$).

Unlike a large number of bacterial PAIs that insert within transfer RNA genes[21], the *E. faecalis* PAI occurs in a non-coding region flanked by an ORF specifying a hypothetical protein with no known homologue or predictable function on one side, and a putative oxidoreductase of unknown function but related to the aldo/keto reductase family, on the other (Fig. 3a). ORFs in the vicinity of the insertion site include those specifying putative ferrous ion transport functions and a glyoxalase family protein, but none that would suggest a known insertion selection mechanism.

Extensive nucleotide sequence identity exists at the 5′ end of the PAI with contiguous conjugation-related structural genes of enterococcal pheromone-responsive plasmids pAM373 and pAD1 (ref. 20). This suggests that at least one-third of the PAI evolved from the integration of such plasmid sequences into the chromosome, although the nucleotide sequence flanking the apparent plasmid-derived regions failed to provide a discernable mechanism for integration. Subsequent divergence apparently arose from the insertion of transposable elements that distance the cytolysin determinants from the conjugation-related structural genes. The only transfer-related genes present, however, are those specifying a TraG-like protein (unknown function) and a region with 87% identity at the nucleotide level to a second transfer origin (*oriT*) recently identified in pAD1 (ref. 20), suggesting the prospect for mobilization of this element from a donor to recipient strain. Filter mating experiments revealed that although the erythromycin-resistant methylase (Erm^r) and gentamicin resistance (Gn^r) determinants could be transferred from MMH594b (donor, derivative of MMH594 with the PAI tagged with a chloramphenicol resistance (Cm^r) determinant) to FA2-2 (plasmid-free recipient, lacking the

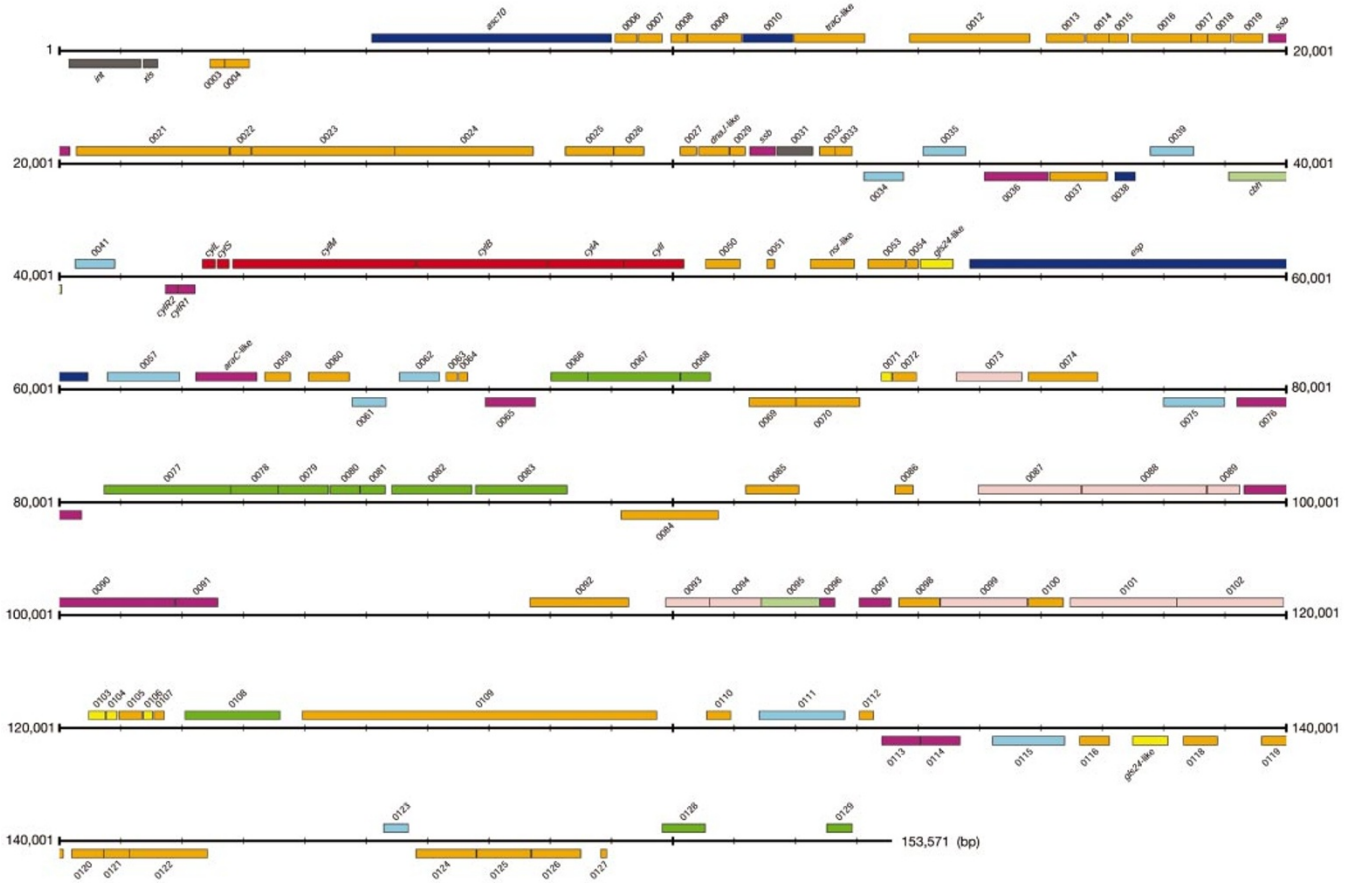

Figure 4 Linear representation of the pathogenicity island in *E. faecalis* MMH594. Coding sequences were defined by combining predictions made by Artemis[29] with visual inspection of ORFs for the presence of start codons and upstream ribosome-binding sites. Potential coding sequences were then subjected to BLASTp similarity searches against the non-redundant protein database. Predicted coding regions transcribed on the forward DNA strand are displayed above the genomic scale line and those transcribed on the reverse DNA strand are displayed below the scale line. Proposed gene name designations or gene identification numbers are presented with each coding region. Colour coding of the ORFs is as follows: dark grey, integrase, excisionase, endonuclease; red, cytolysin operon; dark blue, cell surface associated; orange, hypothetical, conserved hypothetical; light green, lipid metabolism, lipoprotein, bile acid hydrolase; magenta, transcriptional regulator, repressor, single-strand binding protein, signal transduction; light blue, transposase/IS elements, recombinase; dark green, carbohydrate metabolism, modifier; yellow, ribosomal, stress-response; light pink, ABC transporter, ATP-binding.

pathogenicity island) at frequencies of 5.02×10^{-6} and 2.6×10^{-8} per donor cell, respectively, there was no evidence for transfer of the Cm^r marker into FA2-2, suggesting that transfer of the PAI occurs more on an evolutionary scale rather than on a laboratory scale.

Although chromosomal elements bearing some of the hallmarks of PAIs have been identified in *Staphylococcus aureus*[26] and *Streptococcus pneumoniae*[27], these lack several of the features common in PAIs, such as large size, variant G + C content, or known relationship to virulence. The 150-kb PAI identified within multiple antibiotic-resistant pathogenic isolates of *E. faecalis* seems to be the first element from a Gram-positive organism to satisfy all criteria.

At least one of the traits found within this pathogenicity island, Esp, is also highly associated with infection-derived isolates of *E. faecium*. The discovery of a number of ORFs with no assignable function included within the PAI, which are absent from a non-infection-derived isolate and rare in fecal isolates, implicates their contribution to enterococcal survival in the hospital, or in the process of disease transmission or pathogenesis. This PAI, or elements thereof, may be a useful marker for detecting unusually pathogenic enterococcal strains, triggering enhanced infection control procedures within a hospital ward. In addition to known virulence traits coded for by this PAI, the PAI circumscribes a cluster of new genes around which therapeutic interventions may be designed. □

Methods

DNA manipulations

Preparation of enterococcal DNA, analysis by restriction mapping, inverse-PCR, chromosome walking, Southern hybridization, nucleotide sequence determination and alignment was essentially done following previously published[8] and standard protocols[28].

Nucleotide sequence information from strains MMH594 and V586, throughout regions conserved in V583, was obtained by single-pass sequencing and verified by restriction analysis. Custom oligonucleotide primers (Integrated DNA Technologies) based on the emerging nucleotide sequence of strain V583 was used for PCR amplification as well as sequencing of gel-purified PCR amplification products. Takara LA PCR kit (Panvera) was used for all PCR reactions. Nucleotide sequence information from regions unique to strains MMH594 and V586 was obtained by direct sequencing of both strands of PCR products using a primer walking approach. Where necessary, restriction fragments from PCR products were cloned into pBluescript II SK − (Stratagene) and sequenced.

For alignment and comparison of the PAI sequences in the three clinical isolates, overlapping regions (segments 1–19 (Fig. 3b)) of the PAI were amplified from genomic DNA, the amplification product in each case was gel purified, restriction mapped using enzymes *Eco*RI and *Hind*III, and sequenced using a primer walking approach. A total of 219 oligonucleotide primers were used to obtain the nucleotide sequence of the PAI in MMH594 and V586.

Quantitative PCR

For quantitative PCR to estimate the frequency of deletion of the 17,036-bp region from within the PAI in V586, genomic DNA prepared from 9×10^8 colony-forming units

(c.f.u.) of V586 was resuspended in 200 µl of TE buffer. Serial dilutions of 1:1, 1:2.5, 1:5, 1:10 and 1:20 were made in TE buffer and 5 µl aliquots representing the DNA concentrations 875 ng, 700 ng, 350 ng, 175 ng and 87.5 ng were subjected to 40 cycles of PCR amplification with the primer pair L1 (5′-GGAGGACTAACTATCAAGAATATT CGTAC-3′) and R1 (5′-CAGAACGTACGTTATCCCCACTAACCACAGGA-3′). This primer pair amplifies a 2.4-kb region spanning the deletion site only in strain V583. The lowest concentration of V583 template that resulted in a detectable product under the PCR conditions used was 175 pg of template (equivalent to DNA from approx. 2.2×10^3 c.f.u.). A detectable amplification product of similar intensity was obtained from 175 ng of V586 DNA (equivalent to DNA from approx. 2.2×10^6 c.f.u.), demonstrating that the frequency of deletion of the 17,036-bp DNA segment from V586 is approximately 1 in 10^3 cells.

Quantitative PCR to determine the frequency of deletion of the entire PAI was done essentially as described above using primer pair PAI164 (5′-ATGCCATGTTCAGC GAAGTTGCCAATTATC-3′) and PAI167 (5′-GCTGATTTATTATGGTTCTCAGC AATCGCC-3′). The lowest concentration of OG1 DNA (which lacks the PAI) that resulted in an amplified product of 2,121 bp was 20 pg (equivalent to DNA from 2×10^2 c.f.u.). No amplified product was detected when up to 2 µg (equivalent to DNA from 2×10^7 c.f.u.) of genomic DNA from V583, V586 or MMH594 was used as template, indicating that deletion of the entire PAI in these strains occurs at a frequency of less than 1 in 10^5 cells.

Received 31 December 2001; accepted 3 April 2002; doi:10.1038/nature00802.

1. Richards, M. J., Edwards, J. R., Culver, D. H. & Gaynes, R. P. Nosocomial infections in combined medical-surgical intensive care units in the United States. *Infect. Control Hosp. Epidemiol.* **21,** 510–515 (2000).
2. Huycke, M. M., Spiegel, C. A. & Gilmore, M. S. Bacteremia caused by hemolytic, high-level gentamicin-resistant *Enterococcus faecalis*. *Antimicrob. Agents Chemother.* **35,** 1626–1634 (1991).
3. Sahm, D. F. *et al. In vitro* susceptibility studies of vancomycin-resistant *Enterococcus faecalis*. *Antimicrob. Agents Chemother.* **33,** 1588–1591 (1989).
4. Arthur, M. & Courvalin, P. Genetics and mechanisms of glycopeptide resistance in enterococci. *Antimicrob. Agents Chemother.* **37,** 1563–1571 (1993).
5. Jett, B. D., Huycke, M. M. & Gilmore, M. S. Virulence of enterococci. *Clin. Microbiol. Rev.* **7,** 462–478 (1994).
6. Haas, W., Shepard, B. D. & Gilmore, M. S. Two-component regulator of *Enterococcus faecalis* cytolysin responds to quorum-sensing autoinduction. *Nature* **415,** 84–87 (2002).
7. Ike, Y., Hashimoto, H. & Clewell, D. B. Hemolysin of *Streptococcus faecalis* subspecies *zymogenes* contributes to virulence in mice. *Infect. Immun.* **45,** 528–530 (1984).
8. Shankar, V., Baghdayan, A. S., Huycke, M. M., Lindahl, G. & Gilmore, M. S. Infection-derived *Enterococcus faecalis* strains are enriched in *esp*, a gene encoding a novel surface protein. *Infect. Immun.* **67,** 193–200 (1999).
9. Shankar, N. *et al.* Role of *Enterococcus faecalis* surface protein Esp in the pathogenesis of ascending urinary tract infection. *Infect. Immun.* **69,** 4366–4372 (2001).
10. Toledo-Arana, A. *et al.* The enterococcal surface protein, Esp, is involved in *Enterococcus faecalis* biofilm formation. *Appl. Environ. Microbiol.* **67,** 4538–4545 (2001).
11. Willems, R. J. L. *et al.* Variant *esp* gene as a marker of a distinct genetic lineage of vancomycin-resistant *Enterococcus faecium* spreading in hospitals. *Lancet* **357,** 853–855 (2001).
12. Woodford, N., Soltani, M. & Hardy, K. J. Frequency of *esp* in *Enterococcus faecium* isolates. *Lancet* **358,** 584 (2001).
13. Baldassarri, L., Bertuccini, L., Ammendolia, M. G., Gherardi, G. & Creti, R. Variant *esp* gene in vancomycin-sensitive *Enterococcus faecium*. *Lancet* **357,** 1802 (2001).
14. Rouch, D. A., Byrne, M. E., Kong, Y. C. & Skurray, R. A. The *aac*A-*aph*D gentamicin and kanamycin resistance determinant of Tn*4001* from *Staphylococcus aureus*: expression and nucleotide sequence analysis. *J. Gen. Microbiol.* **133,** 3039–3052 (1987).
15. Dodd, H. M., Horn, N. & Gasson, M. J. Characterization of IS*905*, a new multicopy insertion sequence identified in lactococci. *J. Bacteriol.* **176,** 3393–3396 (1994).
16. Fierer, J. & Guiney, D. G. Diverse virulence traits underlying different clinical outcomes of *Salmonella* infection. *J. Clin. Invest.* **107,** 775–780 (2001).
17. Gold, O. G., Jordan, H. V. & van Houte, J. The prevalence of enterococci in the human mouth and their pathogenicity in animal models. *Arch. Oral Biol.* **20,** 473–477 (1975).
18. Ferat, J. L. & Michel, F. Group II self-splicing introns in bacteria. *Nature* **364,** 358–361 (1993).
19. Huang, C. C., Narita, M., Yamagata, T. & Endo, G. Identification of three *mer*B genes and characterization of a broad-spectrum mercury resistance module encoded by a class II transposon of *Bacillus megaterium* strain MB1. *Gene* **239,** 361–366 (1999).
20. Francia, M. V. *et al.* Completion of the nucleotide sequence of the *Enterococcus faecalis* conjugative virulence plasmid pAD1 and identification of a second transfer origin. *Plasmid* **46,** 117–127 (2001).
21. Hacker, J. & Kaper, J. B. Pathogenicity islands and the evolution of microbes. *Annu. Rev. Microbiol.* **54,** 641–679 (2000).
22. Galli, D. & Wirth, R. Comparative analysis of *Enterococcus faecalis* sex pheromone plasmids identifies a single homologous DNA region which codes for aggregation substance. *J. Bacteriol.* **173,** 3029–3033 (1991).
23. Rakita, R. M. *et al. Enterococcus faecalis* bearing aggregation substance is resistant to killing by human neutrophils despite phagocytosis and neutrophil activation. *Infect. Immun.* **67,** 6067–6075 (1999).
24. Rozdzinski, E., Marre, R., Susa, M., Wirth, R. & Muscholl-Silberhorn, A. Aggregation substance-mediated adherence of *Enterococcus faecalis* to immobilized extracellular matrix proteins. *Microb. Pathog.* **30,** 211–220 (2001).
25. Giard, J. C., Rince, A., Capiaux, H., Auffray, Y. & Hartke, A. Inactivation of the stress-and starvation-inducible *gls24* operon has a pleiotrophic effect on cell morphology, stress sensitivity, and gene expression in *Enterococcus faecalis*. *J. Bacteriol.* **182,** 4512–4520 (2000).
26. Novick, R. P., Schlievert, P. & Ruzin, A. Pathogenicity and resistance islands of staphylococci. *Microbes Infect.* **3,** 585–594 (2001).
27. Brown, J. S., Gilliland, S. M. & Holden, D. W. A *Streptococcus pneumoniae* pathogenicity island encoding an ABC transporter involved in iron uptake and virulence. *Mol. Microbiol.* **40,** 572–585 (2001).
28. Sambrook, J., Fritsch, E. F. & Maniatis, T. *Molecular Cloning. A Laboratory Manual* (Cold Spring Harbor Laboratory Press, New York, 1990).
29. Rutherford, K. *et al.* Artemis: sequence visualization and annotation. *Bioinformatics* **16,** 944–945 (2000).

Supplementary Information accompanies the paper on *Nature*'s website (http://www.nature.com/nature).

Acknowledgements

This work was supported by grants from the National Institutes of Health, American Heart Association and Research to Prevent Blindness. We thank M. Carson for help with generating the linear map of the pathogenicity island.

Competing interests statement

The authors declare that they have no competing financial interests.

Correspondence and requests for materials should be addressed to N.S. (e-mail: nathan-shankar@ouhsc.edu).

Subendothelial retention of atherogenic lipoproteins in early atherosclerosis

Kristina Skålén*†, Maria Gustafsson*†, Ellen Knutsen Rydberg*, Lillemor Mattsson Hultén*, Olov Wiklund*, Thomas L. Innerarity‡ & Jan Borén*

* *Wallenberg Laboratory for Cardiovascular Research, Göteborg University, Göteborg S-41345, Sweden*
‡ *Gladstone Institute of Cardiovascular Disease, San Francisco, California 94141-9100, USA*
† *These authors contributed equally to this work*

Complications of atherosclerosis are the most common cause of death in Western societies[1]. Among the many risk factors identified by epidemiological studies, only elevated levels of lipoproteins containing apolipoprotein (apo) B can drive the development of atherosclerosis in humans and experimental animals even in the absence of other risk factors[2]. However, the mechanisms that lead to atherosclerosis are still poorly understood. We tested the hypothesis that the subendothelial retention of atherogenic apoB-containing lipoproteins is the initiating event in atherogenesis[3]. The extracellular matrix of the subendothelium, particularly proteoglycans, is thought to play a major role in the retention of atherogenic lipoproteins[4]. The interaction between atherogenic lipoproteins and proteoglycans involves an ionic interaction between basic amino acids in apoB100 and negatively charged sulphate groups on the proteoglycans[5]. Here we present direct experimental evidence that the atherogenicity of apoB-containing low-density lipoproteins (LDL) is linked to their affinity for artery wall proteoglycans. Mice expressing proteoglycan-binding-defective LDL developed significantly less atherosclerosis than mice expressing wild-type control LDL. We conclude that subendothelial retention of apoB100-containing lipoprotein is an early step in atherogenesis.

Table 1 Mutants of the human apoB100 gene

Recombinant LDL	LDL receptor binding	Proteoglycan binding
Control	Normal	Normal
$W_{4369} \rightarrow Y$	Defective	Normal
$R,K_{3359–3369} \rightarrow S,A$	Defective	Defective
$K_{3363} \rightarrow E$	Normal	Defective
6-GBSM	Defective	Defective